ACS APPLIED MATERIALS & INTERFACES

Research Article

www.acsami.org

Multifunctional Tandem Peptide Modified Paclitaxel-Loaded Liposomes for the Treatment of Vasculogenic Mimicry and Cancer Stem Cells in Malignant Glioma

Yayuan Liu,[†] Ling Mei,[†] Qianwen Yu,[†] Chaoqun Xu,[‡] Yue Qiu,[†] Yuting Yang,[†] Kairong Shi,[†] Qianyu Zhang,[†] Huile Gao,[†] Zhirong Zhang,[†] and Qin He*[,†]

[†]Key Laboratory of Drug Targeting and Drug Delivery Systems, West China School of Pharmacy, Sichuan University, No. 17, Block 3, Southern Renmin Road, Chengdu 610041, China

[‡]Sichuan Academy of Chinese Medicine Sciences, No. 51, Block 4, Southern Renmin Road, Chengdu 610041, China

Supporting Information

ABSTRACT: The chemotherapy of aggressive glioma is usually accompanied by a poor prognosis because of the formation of vasculogenic mimicry (VM) and brain cancer stem cells (BCSCs). VM provided a transporting pathway for nutrients and blood to the extravascular regions of the tumor, and BCSCs were always related to drug resistance and the relapse of glioma. Thus, it is important to evaluate the inhibition effect of antiglioma drug delivery systems on both VM and BCSCs. In this study, paclitaxel-loaded liposomes modified with a multifunctional tandem peptide R8-c(RGD) (R8-c(RGD)-Lip) were used for the treatment of glioma. An in vitro cellular uptake study proved the strongest targeting ability to be that of R8-c(RGD)-Lip to glioma stem cells. Drug loaded R8-c(RGD)-Lip exhibited an efficient antiproliferation effect on BCSCs and could induce the destruction of VM channels in vitro. The following pharmacodynamics study demonstrated that R8-c(RGD)-modified drug-loaded liposomes achieved both anti-VM and anti-BCSC effects in vivo. Finally, no significant cytotoxicity of the blood system or major organs of the drug-loaded liposomes was observed under treatment dosage in the safety evaluation. In conclusion, all of the results proved that R8-c(RGD)-Lip was a safe and efficient antiglioma drug delivery system.

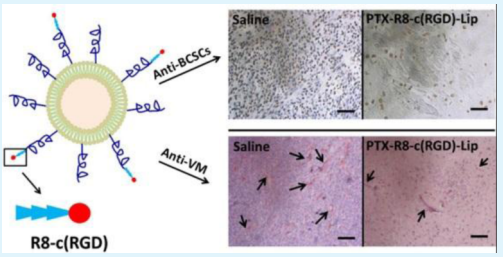

KEYWORDS: *tandem peptide, cell penetrating peptide, vasculogenic mimicry, brain cancer stem cells, antiglioma*

1. INTRODUCTION

Glioma is considered as one of the most aggressive and devastating diseases of the central nervous system, with a median survival of 14.6 months.[1,2] Among all of the therapeutic methods, chemotherapy remains the most commonly used means of glioma treatment.[3,4] However, the chemotherapeutic effect of glioma is often compromised due to several physiologic obstacles. The blood−brain barrier, also known as BBB, represents the first insurmountable barrier for most drugs.[5] As a sanctuary of the central nervous system against invading organisms and unwanted substances, the BBB prevents the intracerebral delivery of almost all exogenous macromolecules and 98% of small-molecule drugs.[6,7] Poor drug penetration thus reduces the potential for antiglioma efficacy. Meanwhile, the existence of vasculogenic mimicry (VM) and brain cancer stem cells (BCSCs) would inevitably lead to a poor prognosis and relapse of glioma. VM was first introduced as a tubular structure to transport erythrocytes and plasma in melanoma.[8] Recent research has confirmed the formation and clinical significance of VM in medulloblastoma and glioblastoma.[9] Unlike the endothelium-lined blood vessels, VM channels were vessel-like structures, formed by malignant tumor cells, which displayed a high degree of plasticity and provided an alternative pathway for nutrient transportation to tumor cells in hypoxic and ischemic areas.[8,10−13] Cancer stem cells, however, were commonly thought to be able to self-renew and differentiate into the heterogeneous cell types that constitute a tumor.[14] BSCSs were one of the first identified cancer stem cells in solid tumors[15,16] and were considered to be responsible for the maintenance and relapse of brain tumors after conventional treatment.[17] Therefore, a superior antiglioma drug delivery system should transport drugs across the BBB, target the tumor foci efficiently, and then undergo combined treatment against both vasculogenic mimicry and brain cancer stem cells.

Up until now, numerous studies had proved that ligand-modified drug-loaded nanocarriers could successfully penetrate the BBB and reach the glioma foci via transport proteins, receptor-mediated transcytosis (RMT), or adsorptive-mediated transcytosis (AMT).[7,18−20] Among all of the ligands, cell-penetrating peptides (CPPs) have recently gained significant importance for drug delivery into the brain.[20−23] These positively charged peptides are capable of penetrating lipidic membranes rapidly via AMT and have been successfully used

Received: May 26, 2015
Accepted: July 15, 2015
Published: July 15, 2015

DOI: 10.1021/acsami.5b04596
ACS Appl. Mater. Interfaces 2015, 7, 16792−16801

for bypassing the P-glycoprotein (P-gp) in the BBB.[24,25] However, the nonspecific penetrating ability greatly limited the application of of CPPs in the systemic administration. In our previous study, we have identified a specific ligand-modified cell-penetrating peptide to overcome this bottleneck.[26] By conjugating cyclic RGD [c(RGD)] to octa-arginine (R8), the cell-penetrating peptide R8 was endowed with the integrin $\alpha_v\beta_3$ binding affinity. Thus, the tandem peptide R8-c(RGD) possessed both selective binding and efficient penetrating capabilities and was proven to be a potential ligand for BBB and glioma targeting. The previous study mainly focused on investigating the improved targeting and penetrating properties of the modified liposome itself. However, the detailed pharmacodynamic study in the previous work is not enough. Therefore, the main point of this study is to further evaluate the antiglioma therapeutic effects and mechanism. By carrying out the pharmacodynamics evaluation against vasculogenic mimicry and brain cancer stem cells, which are both involved in the glioma, we have given a comprehensive understanding of R8-c(RGD)-modified liposomes and proved the synthesized antiglioma therapeutic effects of PTX-loaded R8-c(RGD)-Lip. We studied the targeting efficacy on BCSCs, investigated the inhibition effect of R8-c(RGD)-modified liposomes on VM channels and BCSCs both in vitro and in vivo, and finally carried out a safety evaluation of the modified drug-loaded liposomes.

2. MATERIALS AND METHODS

2.1. Materials and Animals. Peptides with terminal cysteines including R8-c(RGD) peptide [Cys-RRRRRRRR-c(RGDfK), cysteine-modified octa-arginine conjugated to the branch of lysine], cyclic RGD peptide [Cys-c(RGDfK), cysteine conjugated to the branch of lysine], and R8 peptide (Cys-RRRRRRRR) were synthesized according to the standard solid-phase peptide synthesis by ChinaPeptides Co. Ltd. (Shanghai, China). Soybean phospholipids (SPC) and cholesterol were obtained from Shanghai Taiwei Chemical Company (Shanghai, China) and Chengdu Kelong Chemical Company (Chengdu, China), respectively. DSPE-PEG_{2000} and DSPE-PEG_{2000}-Mal were purchased from Shanghai Advanced Vehicle Technology (AVT) LTD Company (Shanghai, China). Paclitaxel (PTX) was purchased from AP Pharmaceutical Co. Ltd. (Chongqing, China). Rabbit anti-integrin α_v, anti-CD133, and anti-GAPDH primary antibodies were purchased from Boster. Horseradish peroxidase (HRP)-labeled goat antirabbit secondary antibody was purchased from ZSGB-BIO (Beijing, China). The 1,2-dioleoyl-*sn*-glycero-3-phosphoethanolamine-*N*-(carboxyfluorescein) (CFPE) used was purchased from Avanti Polar Lipids. The 4′-6-diamidino-2-pheylindole (DAPI) and 3-(4,5-dimethylthiazol-2-yl)-2,5-diphenyltetrazolium bromide (MTT) used were purchased from Beyotime Institute Biotechnology (Haimen, China). BD Matrigel Basement Membrane Matrix was purchased from BD Biosciences (Franklin Lakes, NJ). B27 supplement was purchased from Life Technologies, Thermo Fisher Scientific Inc.. Basic fibroblast growth factor (bFGF) and epidermal growth factor (EGF) were purchased from Shanghai PrimeGene BIO-Tech Co., Ltd. (China). The Annexin V-FITC/propidium iodide (PI) apoptosis detection kit was obtained from KeyGEN Biotech (China). All other chemicals were obtained from commercial sources.

Murine glioma C6 cells was cultured in RPMI-1640 medium (Gibco) supplement with 10% fetal bovine serum (FBS), 100 U/mL penicillin, and 100 μg/mL streptomycin at 37 °C in a humidified 5% CO_2 atmosphere.

BALB/c mice were purchased from West China animal center of Sichuan University (Sichuan, China). All animal experiments were approved by the Experiment Animal Administrative Committee of Sichuan University.

2.2. Preparation of Liposomes. DSPE-PEG_{2000}-R8-c-(RGD), DSPE-PEG_{2000}-RGD, and DSPE-PEG_{2000}-R8 were synthesized as reported before.[26] PEGylated liposomes (PEG-Lip), R8-c(RGD)-modified liposomes [R8-c(RGD)-Lip], R8-modified liposomes (R8-Lip) and RGD-modified liposomes (RGD-Lip) were all prepared through the thin-film hydration method. Briefly, PTX and all of the lipid materials (SPC, cholesterol, DSPE-PEG_{2000}, and differently peptide-modified DSPE-PEG_{2000}) were dissolved in chloroform, and the organic solvent was evaporated to form a lipid film. After being kept in a vacuum overnight, the film was hydrated in phosphate-buffered saline (PBS) at pH 7.4 for 20 min, and the solution was sonicated by a probe sonicator at 80 W for 80 s to form different PTX-loaded liposomes. CFPE-labeled liposomes were prepared by PTX being replaced by the appropriate amount of CFPE. The mean size and ζ potential of different drug-loaded liposomes were measured by Malvern Zetasizer Nano ZS90 (Malvern Instruments Ltd.). The entrapment efficiency (EE%) of PTX was determined by HPLC (Agilent).

2.3. The Culture of C6 Stem Cells. C6 stem cells were cultured through a described protocol.[27] In brief, C6 cells were trypsinized and resuspended with serum-free DMEM culture medium containing 2% B27 supplement, 20 ng/mL bFGF, and 20 ng/mL EGF. The cells were then continuously cultured for 3 weeks until the tumor stem cell spheres were formed. The induced C6 stem cells could then be suspended with serum-containing culture medium again and used for phenotypical identification and further study.

2.4. Western Blot Study. Conventional C6 glioma cells and the induced C6 stem cells were homogenized with cell lysis buffer containing protease inhibitors. The total protein of C6 cells and C6 stem cells was then collected and resolved on 10% SDS-PAGE, and the gels were transferred to polyvinylidene difluoride membranes. The membranes were incubated with rabbit anti-integrin α_v, anti-CD133, or anti-GAPDH primary antibodies, followed by incubation with HRP-labeled goat antirabbit secondary antibodies, and finally detected by Immobilon Western HRP Substrate (Millipore) on a Bio-Rad ChemiDoc MP System (Bio-Rad Laboratories).

2.5. Cellular Uptake Study on BCSCs. C6 stem cells were suspended with serum-containing culture medium, plated in the six-well plates at a density of 5×10^5 cells per well, and allowed to culture for 24 h. CFPE-labeled liposomes were added into the wells at a final CFPE concentration of 1.5 μg/mL for 4 h of cellular uptake. The cells were then washed with cold PBS twice, trypsinized, resuspended, and detected using a flow cytometer (Cytomics FC 500, Beckman Coulter). For qualitative study, gelatin-coated coverslips were preset in the six-well plates, and the C6 stem cells were seeded at a density of 1×10^5 cells per well. After 4 h of incubation with CFPE-labeled liposomes, cells were washed with cold PBS three times, fixed in 4% paraformaldehyde for 30 min, and stained with DAPI for 5 min. The cells were finally imaged by confocal microscope (FV1000, Olympus).

2.6. Destruction of VM Channels. Matrigel-based tube formation assay was carried out to evaluate the formation and destruction of VM channels. A sample of 200 μL of Matrigel

DOI: 10.1021/acsami.5b04596
ACS Appl. Mater. Interfaces 2015, 7, 16792−16801

Table 1. Particle Sizes, ζ Potentials, and PTX Entrapment Efficiency of Different PTX-Loaded Liposomes (n = 3, mean ± SD)

	size (nm)	PDI	ζ potential (mV)	entrapment efficiency (%)
PTX−PEG-Lip	106.3 ± 1.1	0.212 ± 0.031	−6.80 ± 0.66	93.65 ± 2.13
PTX-R8-c(RGD)-Lip	107.6 ± 1.9	0.226 ± 0.022	−2.96 ± 0.80	92.81 ± 5.38
PTX-R8-Lip	102.5 ± 2.3	0.204 ± 0.015	−2.33 ± 0.27	90.94 ± 3.66
PTX-RGD-Lip	100.8 ± 1.5	0.201 ± 0.018	−7.36 ± 0.32	92.37 ± 4.91

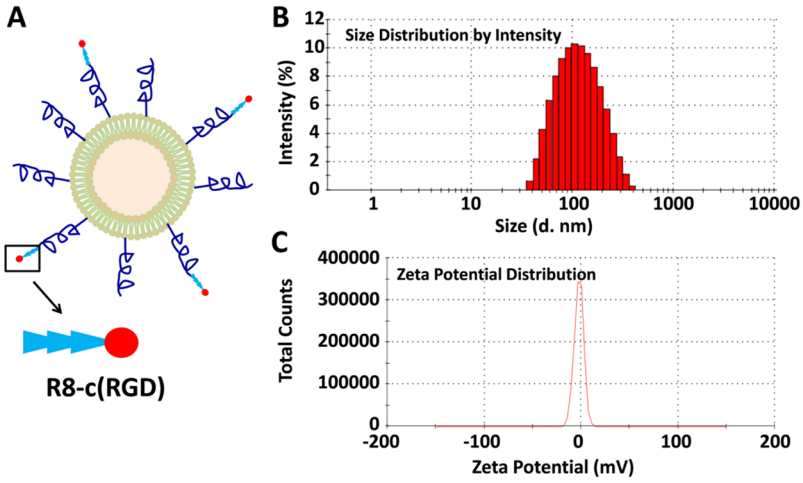

Figure 1. (A) Schematic of R8-c(RGD)-Lip. (B) Size distribution graph of PTX-R8-c(RGD)-Lip. (C) ζ potential distribution graph of PTX-R8-c(RGD)-Lip.

was added into 24-well plates and allowed to solidify under 37 °C for 1 h. C6 cells were plated in the Matrigel-coated wells at a density of 2.5 × 10^5 cells per well. The formation of VM channels was detected and photographed using a Carl Zeiss 40CFL Axiovert 40 inverted microscope (Germany) after 6 and 24 h of incubation.

2.7. Cytotoxicity Study on BCSCs. The cytotoxicity study was evaluated using an MTT assay. Briefly, C6 stem cells were suspended with serum-containing culture medium and plated in the 96-well plates at a density of 2 × 10^3 cells per well. After being cultured for 24 h, different PTX formulations or blank liposomes were added to the wells for another 24 h of incubation. A 20 μL sample of MTT solution (5 mg/mL) was added in the wells. A total of 4 h later, the medium was replaced by 150 μL of dimethyl sulfoxide, and the absorbance was determined at 490 nm with a microplate reader (Thermo Scientific Varioskan Flash).

2.8. Apoptosis Study on BCSCs. For the apoptosis study, C6 stem cells were treated with PTX-loaded liposomes or free PTX at a drug concentration of 1 μg/mL for 24 h. The cells were then collected, washed three times with cold PBS, and incubated with 5 μL of Annexin V-FITC and 5 μL of PI for 15 min in the dark. Finally, the stained cells were analyzed by a flow cytometer (Cytomics FC 500, Beckman Coulter).

2.9. Antiglioma Efficacy. Intracranial glioma models were established on BALB/c mice. Briefly, the mice were anesthetized with 5% chloral hydrate and immobilized on a stereotaxic apparatus. C6 cells (1 × 10^6 cells/5 μL in PBS) were slowly injected into the right brain of each mouse. The mice were then randomly divided into 6 groups including saline, free PTX, PTX−PEG-Lip, PTX-R8-c(RGD)-Lip, PTX-R8-Lip, and PTX-RGD-Lip (n = 11). Saline or PTX formulations were intravenously injected into these glioma-bearing mice via the tail vein at 4, 6, 8, 10, 12, and 14 days after glioma inoculation (PTX dosage of 3 mg/kg). On the 15th day of glioma implantation, one mouse of each group was sacrificed by heart perfusion with PBS and 4% paraformaldehyde, and then the brains were collected for paraffin sections. Hematoxylin and eosin (HE) staining was performed for tumor tissue observation. CD34 and periodic acid−Schiff (PAS) dual staining was used for VM monitoring, and the CD133-based immunoperoxidase method was carried out for BCSCs observation. The survival time of the rest of the mice was recorded and Kaplan−Meier survival curves were plotted for each group.

2.10. In Vivo Safety Evaluation. The safety evaluation of drug-loaded liposomes was carried out using healthy BALB/c mice. A total of 30 mice were divided into 6 groups randomly (n = 5) and were intravenously injected with saline, free PTX, PTX−PEG-Lip, PTX-R8-c(RGD)-Lip, PTX-R8-Lip, or PTX-RGD-Lip at a PTX dosage of 3 mg/kg. The injections were performed every other day for a total of six injections. A total of 24 h after the last injection, the mice were sacrificed, and blood samples were obtained for hematological and biochemistry analysis. For hematological analysis, red blood cells (RBC), white blood cells (WBC), and platelets (PLT) were counted by a MEK-6318K automated hematology analyzer (Nihonkohden, Shinjuku-ku, Japan). As for the biochemical analysis, creatine kinase (CK), aspartate transaminase (AST), alanine aminotransferase (ALT), urea nitrogen (BUN), and creatinine (CREA) levels were measured by a Hitachi 7020 automatic biochemical analyzer (Hitachi Ltd., Hyogo, Japan). Meanwhile, the major organs including heart, liver, spleen, lung, kidney, and brain were also collected for histologic study. HE staining was performed for tissue observation.

2.11. Statistical Analysis. All of the data were presented as mean ± standard deviation. Statistical comparisons were performed by one-way ANOVA for multiple groups, and p values of <0.05 and <0.01 were considered indications of

DOI: 10.1021/acsami.5b04596
ACS Appl. Mater. Interfaces 2015, 7, 16792−16801

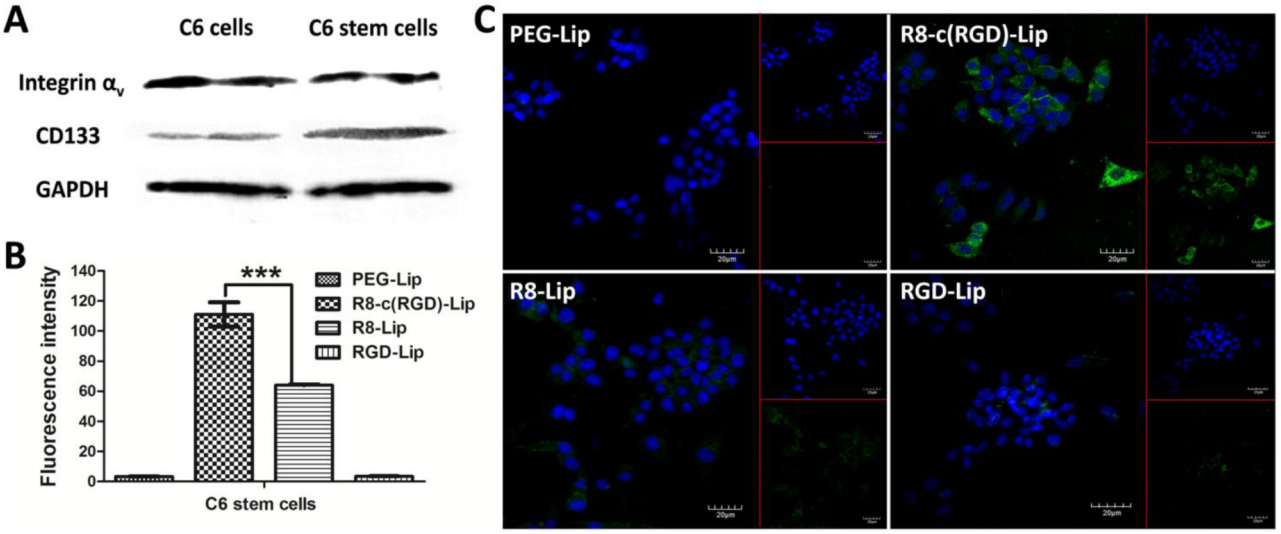

Figure 2. (A) Expression level of integrin α_v and CD133 on C6 cells and C6 stem cells. (B) Results from 4 h of cellular uptake of CFPE-labeled liposomes on C6 stem cells determined by a flow cytometer (n = 3, mean ± SD); *** indicates $p < 0.001$. (C) Confocal images of 4 h of cellular uptake of CFPE-labeled liposomes on C6 stem cells.

statistical difference and statistically significant difference, respectively.

3. RESULTS

3.1. Characterization of Liposomes. Paclitaxel-loaded liposomes (PTX-Lip) with average sizes of less than 110 nm were successfully prepared (Table 1). The polydispersity index (PDI) of all of the liposomes was between 0.2 and 0.3, indicating a uniform distribution of the drug-loaded liposomes. Panels B and C of Figure 1, respectively, exhibited the size and ζ potential distribution graphs of PTX-R8-c(RGD)-Lip. As for the surface charge of different liposomes, it could be seen that the modification of positively charged arginine-containing peptide (R8 and R8-c(RGD)) increased the ζ potential of liposomes from approximately −7 mV to about −3 mV (Table 1). The entrapment efficiency of PTX was higher than 90% in all of the liposome groups.

3.2. Receptor Expression Level. The expression level of CD133 was detected for the phenotypical identification of the in vitro cultured C6 stem cells. Compared to the expression on normal C6 glioma cells, the expression of CD133 on C6 stem cells was significantly increased (Figure 2A), implying the successful induction of brain cancer stem cells in vitro. Meanwhile, as we utilized cyclic RGDfK as the specific binding motif of the tandem peptide (which was widely used for targeting the integrin α_v family overexpressed on different cancer cells including gliomas, melanomas and ovarian carcinomas),[28,29] the expression level of integrin α_v was also measured. C6 cells and C6 stem cells were both integrin α_v-positive expressed cells, and no significant difference of the integrin expression level was observed between them (Figure 2A). However, we have taken a morphological image of C6 stem cells to provide a more sufficient characterization (see Figure S1 in the Supporting Information). The stem cells were shown as monospheres uniformly at diameters of approximately 50−100 μm.

3.3. Cellular Uptake on BCSCs. Cellular uptake on C6 stem cells was measured using CFPE-labeled liposomes to evaluate the targeting efficiency of R8-c(RGD)-Lip to brain cancer stem cells in vitro. As shown in Figure 2B, R8 increased the uptake degree almost 20-fold compared to the results for conventional PEGylated liposomes, while cyclic RGDfK only increased 1.3-fold. The tandem peptide R8-c(RGD) significantly improved the internalization of liposomes on C6 stem cells (by 1.7-fold) compared to the levels in R8-Lip. The qualitative observation of the confocal images showed the same results (Figure 2C). The strongest green fluorescence was observed in the R8-c(RGD)-Lip group. Meanwhile, it could be seen from the staining of DAPI that cancer stem cells exhibited the trend of gathering into clusters during the culture process, which showed the motility and plasticity of cancer stem cells.[30,31] According to the cellular uptake results, the tandem peptide R8-c(RGD) proved the superior brain cancer stem cell targeting ability.

3.4. Cytotoxicity and Apoptosis Study on BCSCs. The cytotoxicity study against brain cancer stem cells was carried out using MTT assay. Given that liposomal drug-delivery systems are known to be biocompatible, the blank liposome vehicles did not show significant cytotoxicity on C6 stem cells as we expected (Figure 3B). The solvent of paclitaxel (ethanol−cremophor ELP 35 mixture, v/v = 1:1) displayed somewhat of an inhibition effect as the concentration increased. However, all of the PTX-loaded liposomes and free PTX exhibited concentration-dependent inhibition effects on C6 stem cells (Figure 3A). Among all of the drug-loaded liposome groups, PTX-R8-c(RGD)-Lip induced the strongest antiproliferation effect on C6 stem cells, indicating that more drug was delivered into the cells. Annexin V−PI dual staining was utilized for the apoptosis study on C6 stem cells. According to the cellular apoptosis dot diagrams (Figure 4 A1−A5), compared to the results for other groups, the distribution of the PTX-R8-c(RGD)-Lip-treated BCSCs displayed a significant upward movement, implying an increased number of late apoptosis and necrotic cells. After 24 h of treatment with PTX−PEG-Lip, PTX-R8-c(RGD)-Lip, PTX-R8-Lip, PTX-RGD-Lip and free PTX, the apoptosis and necrotic rates were 14.00 ± 1.41%, 64.45 ± 4.60%, 25.45 ± 3.04%, 16.45 ± 6.43%, and 20.75 ± 0.77%, respectively (Figure 4B). All of the cytotoxicity and apoptosis studies proved the enhanced inhibition effect of the

DOI: 10.1021/acsami.5b04596
ACS Appl. Mater. Interfaces 2015, 7, 16792−16801

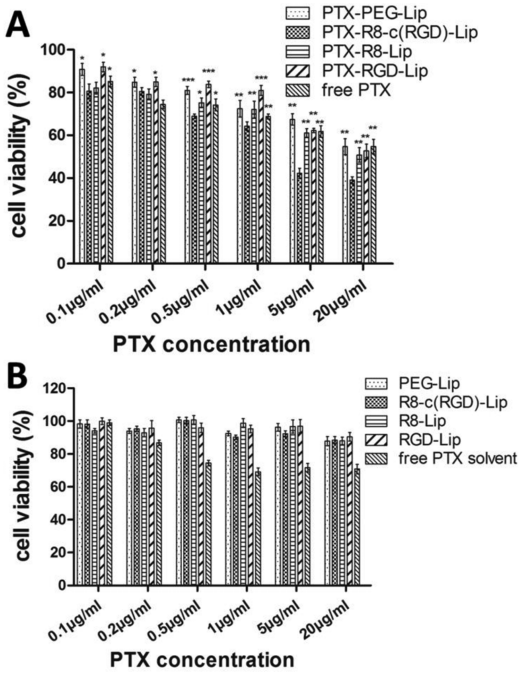

Figure 3. (A) The cytotoxicity study of different PTX formulations on C6 stem cells (n = 3, mean ± SD). *, **, and *** represent $p < 0.05$, $p < 0.01$, and $p < 0.001$ versus the PTX-R8-c(RGD)-Lip group, respectively. (B) The cytotoxicity study of blank liposomes and free PTX solvent on C6 stem cells (n = 3, mean ± SD). The horizontal coordinate represents the corresponding PTX concentrations of blank vehicles.

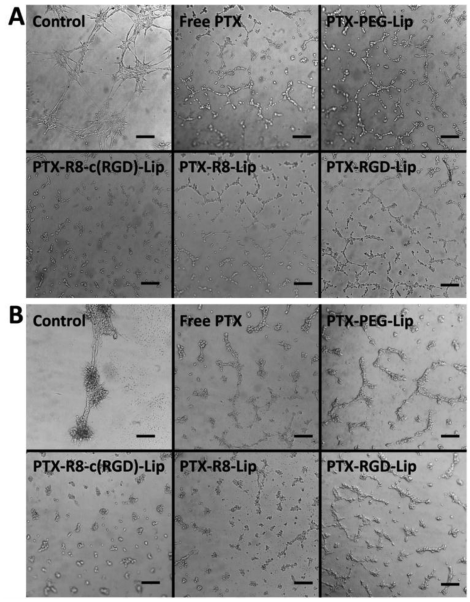

Figure 5. Destruction of C6 VM channels in vitro after 6 h (A) and 24 h (B) of treatment with free PTX or PTX-loaded liposomes; the untreated group was used as the negative control.

R8-c(RGD)-modified PTX-loaded liposomes on brain cancer stem cells in vitro.

3.5. Destruction of VM Channels in Vitro. To carry out the in vitro evaluation of the anti-VM effect of PTX-loaded liposomes, we utilized a reported Matrigel-based tube formation model.[8,27,32] As shown in Figure 5A, the C6 cells without any treatment formed an obvious tube web only 6 h after being seeded onto the Matrigel. The cells then began to gather together, twisted, and finally formed thick tubular structures within 24 h of incubation (Figure 5B). However, when the glioma cells were co-cultured with PTX formulations, the cells only turned into tiny and thin tube analogues, and the formation of these tubelike channels was significantly inhibited. What is more, among all of the PTX-treated groups, only the cells from the PTX-R8-c(RGD)-Lip group failed to aggregate or form connecting nodes, indicating the strongest destruction effect on VM channels of the tandem-peptide-modified drug-loaded liposomes.

3.6. Antiglioma Efficacy. The pharmacodynamics study was carried out to evaluate the antiglioma effects of PTX-loaded

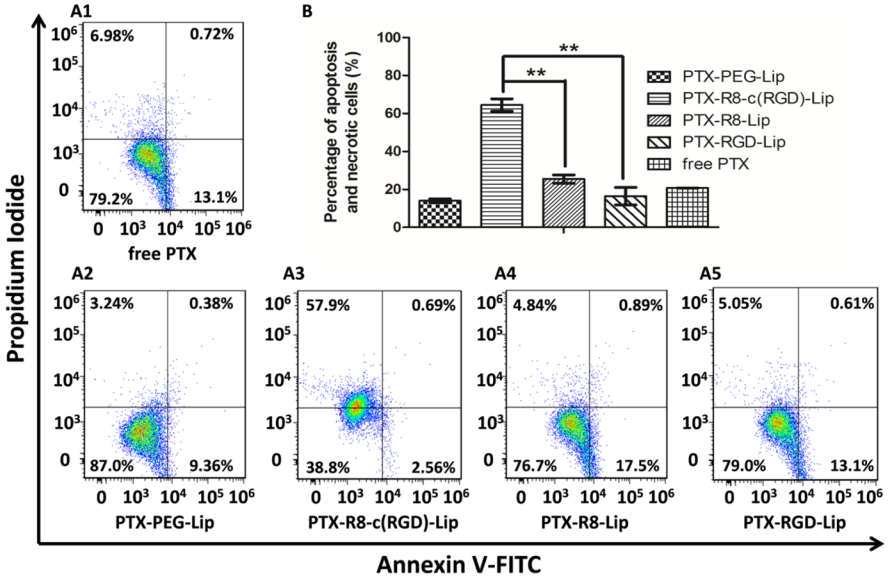

Figure 4. Apoptosis study on C6 stem cells after incubation with free PTX (A1), PTX−PEG-Lip (A2), PTX-R8-c(RGD)-Lip (A3), PTX-R8-Lip (A4), and PTX-RGD-Lip (A5). (B) The percentage of apoptosis and necrotic cells after treatment with different PTX formulations (n = 3, mean ± SD). ** represents $p < 0.01$.

DOI: 10.1021/acsami.5b04596
ACS Appl. Mater. Interfaces 2015, 7, 16792−16801

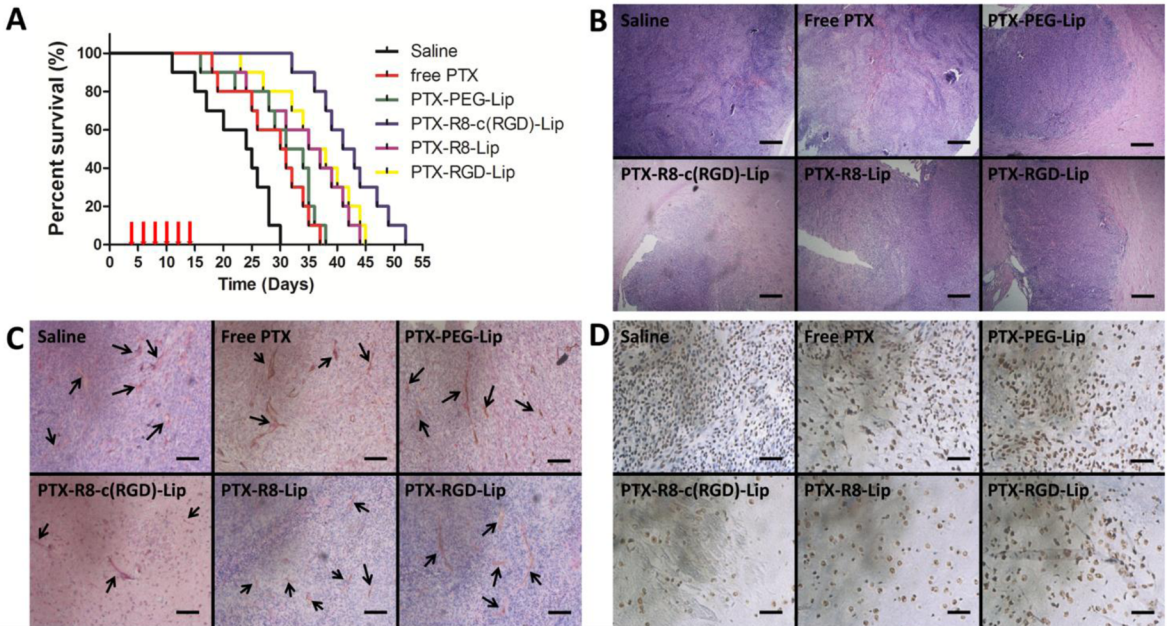

Figure 6. Antiglioma study of PTX-loaded liposomes on intracranial-C6-bearing mice. (A) Kaplan−Meier survival curve of intracranial-C6-glioma-bearing mice treated with different PTX formulations (n = 10). The saline group was used as the negative control. Red arrows indicate the times of treatment. (B) HE staining of brain glioma tissues. Scale bars represent 400 μm. (C) CD34-PAS dual staining of brain glioma tissues. Scale bars represent 200 μm. Black arrows indicate pink vasculogenic mimicry in vivo. (D) CD133 staining of brain glioma tissues. Scale bars represent 50 μm. Brain cancer stem cells with CD133 positive expression were shown in brown.

liposomes. As shown in the Kaplan−Meier survival curves (Figure 6A), the median survival time of the intracranial-glioma-bearing mice was significantly prolonged after six rounds of treatment compared to that of the untreated saline group (24 days). Among all of the PTX-treated groups, the PTX-R8-c(RGD)-Lip group exhibited the most efficient antiglioma effect by prolonging the medium survival time to 43 days, significantly longer than that of the free PTX group (30 days), the PTX−PEG-Lip group (32 days), the PTX-R8-Lip group (35 days), and the PTX-RGD-Lip group (35 days) (Table 2). Several histological analyses at the glioma foci were then utilized to investigate the therapeutic effect of PTX formulations. Figure 6B displayed the hematoxylin−eosin (HE) staining photos. Compared to that of the other groups, a significantly decreased tumor area was observed in the PTX-R8-c(RGD)-Lip group, indicating the enhanced antiproliferation effect induced by the tandem peptide R8-c(RGD) in vivo. CD34 periodic acid−Schiff dual staining was used for the observation of VM channels in vivo. As shown in Figure 6C, pink tubular structures displayed a scattered distribution at the glioma foci, and an obvious reduction of these pink channels could be observed in the PTX-R8-c(RGD)-Lip group. Immunohistochemical CD133 staining was utilized for the identification of brain cancer stem cells. CD133-positive cells were stained in brown, and negative cells were shown in blue. Figure 6D demonstrated a host of BCSCs in the untreated group, and the number of BCSCs greatly decreased after the treatment of PTX-R8-c(RGD)-Lip. Therefore, the tandem peptide R8-c(RGD)-modified paclitaxel-loaded liposomes displayed antiglioma, anti-VM, and anti-BCSCs effects, which would lead to an efficient glioma treatment including tumor inhibition, cutting off the nutrient-transporting channels, and preventing the relapse of glioma.

Table 2. Median Survival Time of the Glioma-Bearing Mice Treated with Different PTX Formulations[a]

group	median (day)	standard error	95% confidence interval	significant results	increased survival time
saline	24	2.0	18.5−26.3	--	--
free PTX	30	2.1	24.7−32.7	a	25%
PTX−PEG-Lip	32	2.2	26.1−34.7	a	33%
PTX-R8-c(RGD)-Lip	43	1.9	38.3−45.9	a,b,c,d,e	79%
PTX-R8-Lip	35	2.7	28.6−39.2	a	46%
PTX-RGD-Lip	35	2.3	31.5−40.5	a	46%

[a]a, $p < 0.05$ versus saline; b, $p < 0.05$ versus free PTX; c, $p < 0.05$ versus PTX−PEG-Lip; d, $p < 0.05$ versus PTX-R8-Lip; e, $p < 0.05$ versus PTX-RGD-Lip).

3.7. Safety Evaluation of Drug-Loaded Liposomes.

Paclitaxel is known for the myelosuppression effect on organisms,[33] and thus the systemic toxicity of drug-loaded liposomes was evaluated here in healthy mice. As shown in Table 3, the free PTX drug-treated mice displayed a significant decrease in WBC compared to the results from the saline group, but none of the liposomal groups showed significant cytotoxicity on the blood system. As for the biomarkers, CK was used as an indicator for the diagnosis of cardiac diseases,[34] AST and ALT were used for the evaluation of liver functions,[35] and the change in BUN and CREA usually indicated kidney injury.[36] According to the data shown in Table 4, the level of AST and ALT exhibited a significant increase in the free PTX group, indicating the potential hepatotoxicity of paclitaxel. However, no obvious influence on any of the serum biomarkers was observed among all of the liposomal treatment groups. The HE staining also demonstrated that all of the main organs

DOI: 10.1021/acsami.5b04596
ACS Appl. Mater. Interfaces 2015, 7, 16792−16801

Table 3. Blood Cell Levels in BALB/c Mice after Treatment with Different PTX Formulations (n = 5)

groups	WBC × 10^9/L[a]	RBC × 10^{12}/L	PLT × 10^9/L
saline	3.98 ± 0.19	7.72 ± 0.99	401 ± 60
free PTX	2.67 ± 0.59[b]	7.22 ± 0.73	404 ± 87
PTX−PEG-Lip	3.70 ± 1.01	8.46 ± 0.51	410 ± 40
PTX-R8-c(RGD)-Lip	3.75 ± 0.23	7.75 ± 0.43	419 ± 49
PTX-R8-Lip	3.32 ± 0.68	7.25 ± 1.36	399 ± 69
PTX-RGD-Lip	3.88 ± 1.91	7.31 ± 0.62	416 ± 71

[a]WBC; white blood cells. RBC: red blood cells. PLT: platelets. [b]p < 0.05 versus saline.

(including the heart, liver, spleen, lung, kidney, and brain) were normal and without obvious histopathological lesions (Figure 7). Thus, all of these results proved the safety and biocompatibility of a liposomal drug delivery system at the treatment dose.

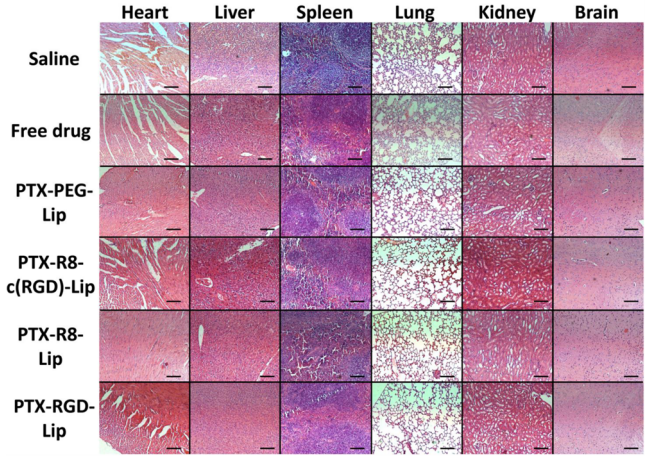

Figure 7. Histological analysis of the different organs of BALB/c mice after treatment with different PTX formulations. Scale bars represent 200 μm.

4. DISCUSSION

In this study, we successfully prepared paclitaxel-loaded liposomes decorated with a tandem peptide, R8-c(RGD). The chemical and physical properties including size, surface charge, and surface chemistry are important factors that determine the pharmacokinetics and biodistribution of nanoparticles.[37] Herein, all of these different modified liposomes were uniformly distributed with high PTX-entrapment efficiency. All of the lipid materials were negatively charged, and the modification amount of peptides in this study was relatively low. Thus, although polyarginine is known to be a positively charged peptide, the ζ potential of R8-containing liposomes was still around −3 mV (Table 1). The weak negatively charged property would benefit the behavior of liposomes in vivo and could avoid the interaction of liposomes with plasma proteins at some degree.[38]

Cell-penetrating peptides, also termed as "Trojan Horses" recently,[39] were famous for their power to break through biobarriers for the mediation of drug delivery into cells and tissues.[39−42] Thus, R8 greatly improved the liposomal uptake on brain cancer stem cells (Figure 2B). In contrast, the modification of cyclic RGD only slightly increased the cellular uptake because these so-called "homing peptides" could just selectively bind to cell surface receptors but exhibited relatively weak internalization properties.[43] Thus, cyclic RGD could not mediate efficient cellular uptake even if the C6 stem cells also overexpress integrin α_v. However, when cyclic RGD was conjugated to acta-arginine to form the tandem peptide R8-c(RGD), the liposomal uptake was further elevated 1.7-fold compared to the results from R8-Lip (Figure 2B). The significant increase demonstrated a synergistic internalization effect of the tandem peptide. When the RGD motif specifically recognized integrin $\alpha_v\beta_3$ on the cancer stem cells, the liposomes were drawn into closer contact with the cell surface, which enhanced the possibility of the R8 domain exerting the penetrating effect.[28,44] The enhanced internalization into brain cancer stem cells would contribute to improve the therapeutic effects both in vitro and in vivo.

Because this study was mainly focused on the treatment of brain cancer stem cells in malignant glioma, a series of pharmacodynamics evaluations in vitro were carried out using the serum-free cultured C6 stem cells; thus, it is necessary to certify the phenotype of the cultured glioma stem cells. The five-transmembrane glycoprotein CD133 (also known as prominin-1) is commonly designated as a marker for identifying cancer stem cells in different tumor types.[14] The increased expression of CD133 on glioma cells is always related with tumorigenic, motility, drug resistance, and poor prognosis.[15,16,45] Figure 2A proved the significantly increased expression level of CD133 on the cultured C6 stem cells in this study, indicating the successful induction of brain cancer stem cells in vitro. When the C6 stem cells were used for cytotoxicity study, we had identified an interesting phenomenon. In the previous research, we have reported the cytotoxicity study of the same PTX-loaded liposomes as used herein on C6 glioma cells.[26] By comparing the antiproliferation effect on conventional glioma cells (in the previously published data) with that on brain cancer stem cells (Figure 3A), it could be observed that the cell viability of C6 stem cells was significant higher than that of C6 cells at the same dosage of the same PTX formulation. This difference resulted from the drug resistance of cancer stem cells. Cancer stem cells were thought to have an important mechanism of multiple drug resistance (MDR).[46,47]

Table 4. Serum Biomarkers in BALB/c Mice after Treatment with Different PTX Formulations (n = 5)

groups	CK (UL)	AST (IU/L)	ALT (IU/L)	BUN (mM)	CREA (μM)
saline	724.3 ± 104.1	190.3 ± 42.8	27.6 ± 10.4	7.1 ± 0.7	5.5 ± 1.1
free PTX	869.3 ± 116.5	253.6 ± 51.7[a]	54.0 ± 9.6[a]	7.9 ± 0.8	6.2 ± 0.5
PTX−PEG-Lip	611.7 ± 160.7	147.6 ± 36.5	36.1 ± 5.1	7.3 ± 0.5	5.5 ± 1.3
PTX-R8-c(RGD)-Lip	648.5 ± 160.8	153.3 ± 55.9	42.3 ± 6.8	8.7 ± 0.4	6.5 ± 1.9
PTX-R8-Lip	783.5 ± 254.3	190.5 ± 39.4	45.5 ± 7.8	7.7 ± 1.1	5.3 ± 1.5
PTX-RGD-Lip	751.7 ± 155.6	160.0 ± 36.4	30.7 ± 7.6	8.6 ± 0.8	5.7 ± 0.9

[a]p < 0.05 versus saline group.

DOI: 10.1021/acsami.5b04596
ACS Appl. Mater. Interfaces 2015, 7, 16792−16801

Many researchers had identified that the ATP-binding cassette (ABC) drug transporters (for example, the most well known ABC transporter P-glycoprotein (P-gp)) have been shown to protect cancer stem cells from chemotherapeutic agents.[47−49] A recent study has confirmed that integrin $\alpha_v\beta_3$ expressed on the cancer stem cells also contributed to the therapeutic resistance.[50]

Another important point of this study was the antiproliferation effect against the vasculogenic mimicry in glioma. Malignant glioma cells exhibited a high degree of plasticity, such that they were easy to differentiate and formed tubelike structures for nutrient transporting to tumor cells in vivo, which was termed as vasculogenic mimicry.[10,12,13] Figure 5 demonstrated the tubular structure formation property of glioma cells on the Matrigel. The R8-c(RGD)-modified drug-loaded liposomes indeed induced the strongest destruction effect on VM channels in vitro. The next in vivo evaluation also certified the efficient anti-VM capability of PTX-R8-c(RGD)-Lip. CD34-PAS dual staining was a commonly used method for VM identification. CD34 was used for the staining of endothelium cells and endothelial vascular tissue, and PAS could identify vascular basement membranes.[13] Thus, as alternative nutrient-transporting channels formed by tumor cells instead of endothelial cells, the VM would act like CD34-negative and PAS-positive channels.[12,13] The amount of VM channels in the glioma foci was significantly decreased after the treatment of PTX-R8-c(RGD)-Lip (Figure 6C). The destruction of vasulogenic mimicry would interrupt the nutrient and blood transporting to the extravascular core region of the tumor, thus leading to the improved antiglioma therapeutic effect.[51,52]

In this study, we have carried out a long-term toxicity evaluation of different PTX formulations. The mice were treated with a therapeutic dose of the drug every other day for a total of six injections. The hematological and biochemical analysis and the histological study then proved the safety of the liposomal formulations. As for the acute toxicity evaluation, we have increased the dose to 15 mg/kg (5-fold compared to the treatment dose) and tried to detect the median lethal dose (LD50) of different PTX formulations. However, as liposomes are known to be biocompatible, no mice died after a single systemic administration within 24 h (data not shown). Due to the relatively low drug-loading rate of liposomes, we are not able to further increase the dose of PTX. Therefore, through both acute and long-term toxicity evaluation, we concluded that the PTX-loaded liposomes were safe and biocompatible, at least at the treatment dose.

5. CONCLUSIONS

In this study, we have investigated the antiglioma effect of paclitaxel-loaded liposomes modified with a multifunctional tandem peptide R8-c(RGD). PTX-R8-c(RGD)-Lip displayed a strong targeting ability to brain cancer stem cells and exhibited an efficient inhibition effect on vasculogenic mimicry and cancer stem cells of glioma, both in vitro and in vivo. In conclusion, all of the results indicated that the R8-c(RGD)-modified liposomes could serve as a potential drug delivery system for antiglioma treatment.

■ ASSOCIATED CONTENT

Supporting Information

The morphological identification of C6 stem cell spheres. The Supporting Information is available free of charge on the ACS Publications website at DOI: 10.1021/acsami.5b04596.

■ AUTHOR INFORMATION

Corresponding Author

*E-mail: qinhe@scu.edu.cn. Tel/Fax: +86 28 85502532.

Notes

The authors declare no competing financial interest.

■ ACKNOWLEDGMENTS

The work was funded by the National Basic Research Program of China (973 Program, 2013CB932504), the National Natural Science Foundation of China (81373337), and the Sichuan Province Infrastructure Platform of Science and Technology (15010116).

■ REFERENCES

(1) Wick, W.; Hartmann, C.; Engel, C.; Stoffels, M.; Felsberg, J.; Stockhammer, F.; Sabel, M. C.; Koeppen, S.; Ketter, R.; Meyermann, R.; et al. NOA-04 Randomized Phase III Trial of Sequential Radiochemotherapy of Anaplastic Glioma with Procarbazine, Lomustine, and Vincristine or Temozolomide. *J. Clin. Oncol.* **2009**, *27* (35), 5874−5880.

(2) Anderson, M. D.; Hamza, M. A.; Hess, K. R.; Puduvalli, V. K. Implications of Bevacizumab Discontinuation in Adults with Recurrent Glioblastoma. *Neuro. Oncol.* **2014**, *16* (6), 823−828.

(3) Bhujbal, S. V.; de Vos, P.; Niclou, S. P. Drug and Cell Encapsulation: Alternative Delivery Options for the Treatment of Malignant Brain Tumors. *Adv. Drug Delivery Rev.* **2014**, *67*, 142−153.

(4) Cheng, Y.; Morshed, R. A.; Auffinger, B.; Tobias, A. L.; Lesniak, M. S. Multifunctional Nanoparticles for Brain Tumor Imaging and Therapy. *Adv. Drug Delivery Rev.* **2014**, *66*, 42−57.

(5) Kreuter, J. Drug Delivery to the Central Nervous System by Polymeric Nanoparticles: What do we Know? *Adv. Drug Delivery Rev.* **2014**, *71*, 2−14.

(6) Yan, H.; Wang, L.; Wang, J.; Weng, X.; Lei, H.; Wang, X.; Jiang, L.; Zhu, J.; Lu, W.; Wei, X.; Cong, L. Two-Order Targeted Brain Tumor Imaging by Using an Optical/Paramagnetic Nanoprobe Across the Blood Brain Barrier. *ACS Nano* **2011**, *6* (1), 410−420.

(7) Chen, Y.; Liu, L. Modern Methods for Delivery of Drugs Across the Blood−Brain Barrier. *Adv. Drug Delivery Rev.* **2012**, *64* (7), 640−665.

(8) Ling, G.; Wang, S.; Song, Z.; Sun, X.; Liu, Y.; Jiang, X.; Cai, Y.; Du, M.; Ke, Y. Transforming Growth Factor-b is Required for Vasculogenic Mimicry Formation in Glioma Cell Line U251MG. *Cancer Biol. Ther.* **2011**, *12* (11), 978−988.

(9) Huang, M.; Ke, Y.; Sun, X.; Yu, L.; Yang, Z.; Zhang, Y.; Du, M.; Wang, J.; Liu, X.; Huang, S. Mammalian Target of Rapamycin Signaling is Involved in the Vasculogenic Mimicry of Glioma via Hypoxia-Inducible Factor-1α. *Oncol. Rep.* **2014**, *32* (5), 1973−1980.

(10) Chen, Y.; Jing, Z.; Luo, C.; Zhuang, M.; Xia, J.; Chen, Z.; Wang, Y. Vasculogenic Mimicry−Potential Target for Glioblastoma Therapy: an in Vitro and in Vivo Study. *Med. Oncol.* **2012**, *29* (1), 324−331.

(11) Kirschmann, D. A.; Seftor, E. A.; Hardy, K. M.; Seftor, R. E.; Hendrix, M. J. Molecular Pathways: Vasculogenic Mimicry in Tumor Cells: Diagnostic and Therapeutic Implications. *Clin. Cancer Res.* **2012**, *18* (10), 2726−2732.

(12) Chen, Y.-S.; Chen, Z.-P. Vasculogenic Mimicry: a Novel Target for Glioma Therapy. *Aizheng* **2014**, *33* (2), 74.

(13) Liu, X.-m.; Zhang, Q.-p.; Mu, Y.-g.; Zhang, X.-h.; Sai, K.; Pang, J. C.-S.; Ng, H.-K.; Chen, Z.-p. Clinical Significance of Vasculogenic Mimicry in Human Gliomas. *J. Neuro-Oncol.* **2011**, *105* (2), 173−179.

DOI: 10.1021/acsami.5b04596
ACS Appl. Mater. Interfaces 2015, 7, 16792−16801

(14) Sarvi, S.; Mackinnon, A. C.; Avlonitis, N.; Bradley, M.; Rintoul, R. C.; Rassl, D. M.; Wang, W.; Forbes, S. J.; Gregory, C. D.; Sethi, T. CD133+ Cancer Stem-Like Cells in Small Cell Lung Cancer are Highly Tumorigenic and Chemoresistant but Sensitive to a Novel Neuropeptide Antagonist. *Cancer Res.* **2014**, *74* (5), 1554−1565.
(15) Singh, S. K.; Clarke, I. D.; Terasaki, M.; Bonn, V. E.; Hawkins, C.; Squire, J.; Dirks, P. B. Identification of a Cancer Stem Cell in Human Brain Tumors. *Cancer Res.* **2003**, *63* (18), 5821−5828.
(16) Singh, S. K.; Hawkins, C.; Clarke, I. D.; Squire, J. A.; Bayani, J.; Hide, T.; Henkelman, R. M.; Cusimano, M. D.; Dirks, P. B. Identification of Human Brain Tumour Initiating Cells. *Nature* **2004**, *432* (7015), 396−401.
(17) Zhu, Z.; Khan, M. A.; Weiler, M.; Blaes, J.; Jestaedt, L.; Geibert, M.; Zou, P.; Gronych, J.; Bernhardt, O.; Korshunov, A.; et al. Targeting Self-Renewal in High-Grade Brain Bumors Leads to Loss of Brain Tumor Stem Cells and Prolonged Survival. *Cell stem cell* **2014**, *15* (2), 185−198.
(18) Chen, H.; Tang, L.; Qin, Y.; Yin, Y.; Tang, J.; Tang, W.; Sun, X.; Zhang, Z.; Liu, J.; He, Q. Lactoferrin-Modified Procationic Liposomes as a Novel Drug Carrier for Brain Delivery. *Eur. J. Pharm. Sci.* **2010**, *40* (2), 94−102.
(19) Li, J.; Zhou, L.; Ye, D.; Huang, S.; Shao, K.; Huang, R.; Han, L.; Liu, Y.; Liu, S.; Ye, L.; et al. Choline−Derivate-Modified Nanoparticles for Brain-Targeting Gene Delivery. *Adv. Mater.* **2011**, *23* (39), 4516−4520.
(20) Qin, Y.; Chen, H.; Yuan, W.; Kuai, R.; Zhang, Q.; Xie, F.; Zhang, L.; Zhang, Z.; Liu, J.; He, Q. Liposome Formulated with TAT-Modified Cholesterol for Enhancing the Brain Delivery. *Int. J. Pharm.* **2011**, *419* (1), 85−95.
(21) Hervé, F.; Ghinea, N.; Scherrmann, J.-M. CNS Delivery via Adsorptive Transcytosis. *AAPS J.* **2008**, *10* (3), 455−472.
(22) Qin, Y.; Chen, H.; Zhang, Q.; Wang, X.; Yuan, W.; Kuai, R.; Tang, J.; Zhang, L.; Zhang, Z.; Zhang, Q.; et al. Liposome Formulated with TAT-Modified Cholesterol for Improving Brain Delivery and Therapeutic Efficacy on Brain Glioma in Animals. *Int. J. Pharm.* **2011**, *420* (2), 304−312.
(23) Gong, C.; Li, X.; Xu, L.; Zhang, Y.-H. Target Delivery of a Gene into the Brain Using the RVG29-Oligoarginine Peptide. *Biomaterials* **2012**, *33* (12), 3456−3463.
(24) Rousselle, C.; Clair, P.; Lefauconnier, J.-M.; Kaczorek, M.; Scherrmann, J.-M.; Temsamani, J. New Advances in the Transport of Doxorubicin Through the Blood-Brain Barrier by a Peptide Vector-Mediated Strategy. *Mol. Pharmacol.* **2000**, *57* (4), 679−686.
(25) Deshayes, S.; Morris, M.; Divita, G.; Heitz, F. Cell-Penetrating Peptides: Tools for Intracellular Delivery of Therapeutics. *Cell. Mol. Life Sci.* **2005**, *62* (16), 1839−1849.
(26) Liu, Y.; Ran, R.; Chen, J.; Kuang, Q.; Tang, J.; Mei, L.; Zhang, Q.; Gao, H.; Zhang, Z.; He, Q. Paclitaxel Loaded Liposomes Decorated with a Multifunctional Tandem Peptide for Glioma Targeting. *Biomaterials* **2014**, *35* (17), 4835−4847.
(27) Li, X.-Y.; Zhao, Y.; Sun, M.-G.; Shi, J.-F.; Ju, R.-J.; Zhang, C.-X.; Li, X.-T.; Zhao, W.-Y.; Mu, L.-M.; Zeng, F.; et al. Multifunctional Liposomes Loaded with Paclitaxel and Artemether for Treatment of Invasive Brain Glioma. *Biomaterials* **2014**, *35* (21), 5591−5604.
(28) Kibria, G.; Hatakeyama, H.; Ohga, N.; Hida, K.; Harashima, H. Dual-Ligand Modification of PEGylated Liposomes Shows Better Cell Selectivity and Efficient Gene Delivery. *J. Controlled Release* **2011**, *153* (2), 141−148.
(29) Vachutinsky, Y.; Oba, M.; Miyata, K.; Hiki, S.; Kano, M. R.; Nishiyama, N.; Koyama, H.; Miyazono, K.; Kataoka, K. Antiangiogenic Gene Therapy of Experimental Pancreatic Tumor by SFlt-1 Plasmid DNA Carried by RGD-Modified Crosslinked Polyplex Micelles. *J. Controlled Release* **2011**, *149* (1), 51−57.
(30) Cabrera, M. C.; Hollingsworth, R. E.; Hurt, E. M.; Hurt, E.; Way, O. M. Cancer Stem Cell Plasticity and Tumor Hierarchy. *World J. Stem Cells* **2015**, *7* (1), 27−36.
(31) Leong, H. S.; Chong, F. T.; Sew, P. H.; Lau, D. P.; Wong, B. H.; Teh, B.-T.; Tan, D. S.; Iyer, N. G. Targeting Cancer Stem Cell Plasticity Through Modulation of Epidermal Growth Factor and Insulin-Like Growth Factor Receptor Signaling in Head and Neck Squamous Cell Cancer. *Stem Cells Transl. Med.* **2014**, *3* (9), 1055−1065.
(32) Ju, R.-J.; Li, X.-T.; Shi, J.-F.; Li, X.-Y.; Sun, M.-G.; Zeng, F.; Zhou, J.; Liu, L.; Zhang, C.-X.; Zhao, W.-Y.; et al. Liposomes, Modified with PTD HIV-1 Peptide, Containing Epirubicin and Celecoxib, to Target Vasculogenic Mimicry Channels in Invasive Breast Cancer. *Biomaterials* **2014**, *35* (26), 7610−7621.
(33) Karlsson, M. O.; Molnar, V.; Bergh, J.; Freijs, A.; Larsson, R. A General Model for Time-Dissociated Pharmacokinetic-Pharmacodynamic Relationships Exemplified by Paclitaxel Myelosuppression. *Clin. Pharmacol. Ther.* **1998**, *63* (1), 11−25.
(34) Goldberg, D.; Winfield, D. Diagnostic Accuracy of Serum Enzyme Assays for Myocardial Infarction in a General Hospital Population. *Heart* **1972**, *34* (6), 597.
(35) Ozer, J. S.; Chetty, R.; Kenna, G.; Palandra, J.; Zhang, Y.; Lanevschi, A.; Koppiker, N.; Souberbielle, B. E.; Ramaiah, S. K. Enhancing the Utility of Alanine Aminotransferase as a Reference Standard Biomarker for Drug-Induced Liver Injury. *Regul. Toxicol. Pharmacol.* **2010**, *56* (3), 237−246.
(36) Xin, H.; Sha, X.; Jiang, X.; Zhang, W.; Chen, L.; Fang, X. Anti-Glioblastoma Efficacy and Safety of Paclitaxel-Loading Angiopep-Conjugated Dual Targeting PEG-PCL Nanoparticles. *Biomaterials* **2012**, *33* (32), 8167−8176.
(37) Li, S.-D.; Huang, L. Pharmacokinetics and Biodistribution of Nanoparticles. *Mol. Pharmaceutics* **2008**, *5* (4), 496−504.
(38) Gao, H.; He, Q. The Interaction of Nanoparticles with Plasma Proteins and the Consequent Influence on Nanoparticles Behavior. *Expert Opin. Drug Delivery* **2014**, *11* (3), 409−20.
(39) Huang, Y.; Jiang, Y.; Wang, H.; Wang, J.; Shin, M. C.; Byun, Y.; He, H.; Liang, Y.; Yang, V. C. Curb Challenges of the "Trojan Horse" Approach: Smart Strategies in Achieving Effective yet Safe Cell-Penetrating Peptide-Based Drug Delivery. *Adv. Drug Delivery Rev.* **2013**, *65* (10), 1299−1315.
(40) Milletti, F. Cell-Penetrating Peptides: Classes, Origin, and Current Landscape. *Drug Discovery Today* **2012**, *17* (15), 850−860.
(41) Zhang, Q.; Tang, J.; Fu, L.; Ran, R.; Liu, Y.; Yuan, M.; He, Q. A pH-Responsive α-Helical Cell Penetrating Peptide-Mediated Liposomal Delivery System. *Biomaterials* **2013**, *34* (32), 7980−7993.
(42) Gu, B.; Xie, C.; Zhu, J.; He, W.; Lu, W. Folate-PEG-CKK2-DTPA, a Potential Carrier for Lymph-Metastasized Tumor Targeting. *Pharm. Res.* **2010**, *27* (5), 933−942.
(43) Svensen, N.; Walton, J. G.; Bradley, M. Peptides for Cell-Selective Drug Delivery. *Trends Pharmacol. Sci.* **2012**, *33* (4), 186−192.
(44) Wen, Y.; Roudebush, S. L.; Buckholtz, G. A.; Goehring, T. R.; Giannoukakis, N.; Gawalt, E. S.; Meng, W. S. Coassembly of Amphiphilic Peptide EAK16-II with Histidinylated Analogues and Implications for Functionalization of β-Sheet Fibrils in Vivo. *Biomaterials* **2014**, *35* (19), 5196−5205.
(45) de Mendoza, F. H.; Rodriguez, E. A. Cancer Stem Cells in Brain Tumors. In *Stem Cells in Cancer: Should We Believe or Not?*; Springer: New York, 2014; pp 229−243.
(46) Raha, D.; Wilson, T. R.; Peng, J.; Peterson, D.; Yue, P.; Evangelista, M.; Wilson, C.; Merchant, M.; Settleman, J. The Cancer Stem Cell Marker Aldehyde Dehydrogenase is Required to Maintain a Drug-Tolerant Tumor Cell Subpopulation. *Cancer Res.* **2014**, *74* (13), 3579−3590.
(47) Dean, M.; Fojo, T.; Bates, S. Tumour Stem Cells and Drug Resistance. *Nat. Rev. Cancer* **2005**, *5* (4), 275−284.
(48) Donnenberg, V. S.; Donnenberg, A. D. Multiple Drug Resistance in Cancer Revisited: the Cancer Stem Cell Hypothesis. *J. Clin. Pharmacol.* **2005**, *45* (8), 872−877.
(49) Mallini, P.; Lennard, T.; Kirby, J.; Meeson, A. Epithelial-to-Mesenchymal Transition: What is the Impact on Breast Cancer Stem Cells and Drug Resistance. *Cancer Treat. Rev.* **2014**, *40* (3), 341−348.
(50) Kannan, N.; Nguyen, L. V.; Eaves, C. J. Integrin [beta] 3 Links Therapy Resistance and Cancer Stem Cell Properties. *Nat. Cell Biol.* **2014**, *16* (5), 397−399.

DOI: 10.1021/acsami.5b04596
ACS Appl. Mater. Interfaces 2015, 7, 16792−16801

(51) Itzhaki, O.; Greenberg, E.; Shalmon, B.; Kubi, A.; Treves, A. J.; Shapira-Frommer, R.; Avivi, C.; Ortenberg, R.; Ben-Ami, E.; Schachter, J.; et al. Nicotinamide Inhibits Vasculogenic Mimicry, an Alternative Vascularization Pathway Observed in Highly Aggressive Melanoma. *PLoS One* **2013**, *8* (2), e57160.
(52) Wang, H.; Sun, W.; Zhang, W.-Z.; Ge, C.-Y.; Zhang, J.-T.; Liu, Z.-Y.; Fan, Y.-Z. Inhibition of Tumor Vasculogenic Mimicry and Prolongation of Host Survival in Highly Aggressive Gallbladder Cancers by Norcantharidin via Blocking the Ephrin Type a Receptor 2/Focal Adhesion Kinase/Paxillin Signaling Pathway. *PLoS One* **2014**, *9* (5), e96982.

DOI: 10.1021/acsami.5b04596
ACS Appl. Mater. Interfaces 2015, 7, 16792−16801